UNIVERSITY OF LATVIA

FACULTY OF PHYSICS, MATHEMATICS AND OPTOMETRY

Raitis Grzibovskis

REQUIREMENTS FOR ENERGY LEVEL DETERMINATION OF ORGANIC MATERIALS USING PHOTOELECTRON YIELD SPECTROSCOPY AND SCANNING KELVIN PROBE

SUMMARY OF DOCTORAL THESIS

Submitted for the degree of Doctor of Physics
Subfield: Solid State Physics

Riga, 2019

The doctoral thesis was carried out in the Institute of Solid state physics, University of Latvia, from 2013 to 2019.

The thesis contains an introduction, three chapters, thesis, and reference list.

Form of the thesis: dissertation.

Scientific supervisor: *Dr. phys.* **Aivars Vembris**, senior researcher at the Institute of Solid State Physics, University of Latvia.

Reviewers:

1) *Dr. chem.* **Gunars Bajars**, Institute of Solid State Physics, University of Latvia;
2) Asoc. prof., *Dr. chem.* **Donats Erts**, University of Latvia;
3) Prof., *Dr. habil. phys.* **Vidmantas Gulbinas**, Center for Physical Sciences and Technology, Vilnius, Lithuania.

The thesis will be defended at the public session of the Doctoral Committee of Physics, Astronomy and Mechanics, University of Latvia, at 10.00 on June 21, 2019, in the conference hall of the Institute of Solid state physics, University of Latvia, 8 Kengaraga Street, Riga, Latvia.

The doctoral thesis and its summary are available at the Library of the University of Latvia (19 Raina Blvd, Riga) and the University of Latvia Academic Library (10 Rupniecibas street, Riga).

Chairman
of the Doctoral Committee: Prof., *Dr. habil. phys.* Uldis Rogulis

Secretary
of the Doctoral Committee: Laureta Busevica

ISBN 978-9934-18-448-2

ABSTRACT

More and more often in such devices like photovoltaic cells or light emitting diodes, the classical inorganic materials are being substituted by the organic materials. A huge variety of materials, a molecular design which allows to control and improve the properties of the material, as well as the possibility to manufacture devices using wet casting methods thus decreasing the cost, are advantages that make the organic materials an attractive field to the materials science. Such properties as light absorption, an electrical conductivity, charge carrier mobility, efficiency and wavelength of luminescence, will mainly determine the potential use of the material. The performance of the device will depend not only on the material itself but also on the compatibility between all the materials in the device. As the devices made of organic materials mostly consist of several layers (electron or hole transport layers, the electron or hole blocking layers, an active layer which consists of the mixture of two or more materials, electrodes), the compatibility of materials becomes especially significant. Most directly it is related to the energy levels of materials. Energy level alignment between different layers can diminish the losses in the device and improve its performance. This is the reason why easy and relatively simple methods for energy level and their changes determination are needed.

Ultraviolet photoelectron spectroscopy is the most often used method for energy level determination. However, it is an expensive and complicated method. Substitution with simpler yet less often used methods – photoelectron yield spectroscopy and scanning Kelvin probe – could be possible.

The experimental setup for molecule ionization energy determination using photoelectron yield spectroscopy was built. This method was used to determine the ionization energy of the materials, in the studies of the electrode-organic compound and the organic compound – organic compound interface. Organic compound – organic compound interface studies were made for classical planar structures, as well as for bulk heterojunction systems, which to the best of our knowledge has not been done yet. The results, as well as the conclusions about the advantages and disadvantages of such a method, are shown.

A surface potential using scanning Kelvin probe was obtained for various materials (metals, organic semiconductors, and organic dielectric materials). The obtained results show that the surface potential dependence on metal work function changes with the film thickness and the electrical conductivity of the material.

Keywords: organic materials, energy levels, interfaces, photoelectron emission, Kelvin probe.

CONTENTS

1 INTRODUCTION 6
1.1 Motivation 6
1.2 The aim of the work 6
1.3 Author's contribution 7
1.4 Scientific novelty 7

2 REVIEW OF LITERATURE 8
2.1 Metal-organic compound system studies using UPS 8
2.2 Organic compound – organic compound system studies using UPS 8
2.3 Molecule ionization energy determination using PYS 10
2.4 Scanning Kelvin probe 11

3 EXPERIMENTAL PART 13
3.1 Methods for the production of the samples 13
3.1.1 Wet casting method 13
3.1.2 Thermal evaporation in vacuum 13
3.1.3 Preparation of the substrates (etching of ITO) 13
3.2 Experimental methods and equipment 14
3.2.1 Ionization energy measurements 14
3.2.2 Photoconductivity measurements 15
3.2.3 Surface potential measurements 16
3.2.4 Absorption spectra measurements 17
3.2.5 4-probe method for determination of electrical conductivity 17
3.2.6 Film thickness measurements 18
3.2.7 Scanning electron microscope measurements 18
3.2.8 Photovoltaic effect measurements 18

4 RESULTS AND DISCUSSION 20
4.1 Photoelectrical measurements of pyranilidene fragment containing compounds 20
4.1.1 Energy level determination 20
4.1.2 Photovoltaic effect measurements 22
4.1.3 Conclusions 24
4.2 Studies of the electrode-organic compound interface 24
4.2.1 Conclusions 28

4.3 Studies of the organic compound–organic compound interface 29
4.3.1 Planar heterojunction 29
4.3.2 Bulk heterojunction 30
4.3.3 Conclusions 35
4.4 Surface potential measurements 35
4.4.1 Conclusions 39
THESIS 40
REFERENCES 41
AUTHOR'S PUBLICATIONS 44
Related to the thesis 44
Unrelated to the thesis 44
PARTICIPATION IN CONFERENCES 46
ACKNOWLEDGMENTS 48

1 INTRODUCTION

1.1 Motivation

The vast variety of organic materials, possibility to control the properties of the material by changing the structure of molecule, and the possibility to use wet casting methods determine the increasing popularity of organic materials in the production of various devices, such as organic light emitting diodes (OLED) and organic photovoltaic (OPV) cells. The performance of these devices will be determined not only by the organic material alone but by the compatibility between all of the used materials. OLEDs [1, 2] and OPV cells [3] mostly consist of electrodes, hole and electron injection and transport layers, and active medium, where two compounds are often mixed together. The thickness of such layers is only up to 100 nm [4–7]. Energy level compatibility between different layers allows decreasing the losses in the device and improving its efficiency. That is why fast and relatively simple methods for material energy level and their shift at the metal-organic compound and organic compound–organic compound (OC-OC) interface determination are required. The most popular method for molecule ionization energy and material Fermi level determination of organic materials is ultraviolet photoelectron spectroscopy (UPS). Nevertheless, this method is expensive and complicated as the measurements are carried out in an ultra-high vacuum. Because of this, there is a need for simpler alternative methods, for example, molecule ionization energy can be determined by photoelectron yield spectroscopy (PYS). Its applicability in the energy level shift determination at the metal-organic compound and OC-OC interface has not been widely studied.

The Fermi energy level of organic materials could be determined using scanning Kelvin probe. Yet, there have not been systematic research to show the applicability of this method and to describe the obtained results when measuring the surface potential of organic materials.

1.2 The aim of the work

The aim of the work was to evaluate the applicability of alternative methods which could replace the ultraviolet photoelectron spectroscopy measurements in molecule energy level and their shift determination.

To reach the aim, the following tasks were set:

- To create a photoelectron yield spectroscopy measurement system in the Laboratory of Organic Materials, Institute of Solid state physics;
- To determine the applicability of PYS for molecule energy level determination;

- To acknowledge the applicability of this method in the metal – organic compound interface studies;
- To determine the applicability of PYS in the studies of OC-OC systems (planar and bulk heterojunction);
- To determine the potential of scanning Kelvin probe in the energy level determination.

1.3 Author's contribution

The author has prepared all the investigated samples with spin-coating or thermal evaporation in vacuum method, depending on the properties of the studied material. The author has carried out all of the photoelectrical – photoelectron emission, photoconductivity, and photovoltaic – measurements, as well as the surface potential measurements using scanning Kelvin probe and electrical conductivity measurements using four probe method. Author of this work has characterized samples by thickness measurements using a surface profiler, and thin film absorption measurements.

The author has created a photoelectron yield spectroscopy measurement system in the Laboratory of Organic Materials, Institute of Solid State Physics and made software for this measurement system. Additionally, a measurement system and software for photoconductivity measurements were upgraded.

The author has processed the obtained data and analyzed the results. The obtained results have been presented in local and international conferences, as well as have been published in scientific journals.

1.4 Scientific novelty

In this work photoelectrical properties of pyranilidene containing fragment compounds have been studied. The applicability of these materials in Solar cell creation has been evaluated.

Molecule ionization energy measurements for two indandione derivative's thin films with different morphology were done using photoelectron yield spectroscopy. The ionization energy dependence on film thickness was obtained. Issues related to the measurements of such systems have been discussed.

Energy level shift at the organic compound – organic compound interface of polymer and fullerene derivative samples have been studied. It has been done in planar as well as in bulk heterojunction systems. For the first time, PYS has been applied to the bulk heterojunction system. The obtained results are compared to the UPS measurements.

Systematic studies of the surface potential dependence on the metal work function in Kelvin probe measurements have been done. Surface potential dependence on films thickness was obtained. The results have been linked to the electrical conductivity of the studied material.

2 REVIEW OF LITERATURE

2.1 Metal-organic compound system studies using UPS

UPS is the most popular photoelectron emission method used in the studies of organic materials. It gives information about molecule ionization energy, Fermi level, and energy level shifts at the metal-organic compound interface [8–12].

Often in the UPS measurements increasingly thick organic material film is grown on the metal electrode, using thermal evaporation in a vacuum. At each thickness photoelectron emission spectrum is measured, thus obtaining energy level dependence on film thickness [13]. In the case of polymers, the samples are made using wet casting methods, for example, spin-coating. In this case, the series of samples are made and energy level dependence on film thickness is obtained [14]. Mostly the samples where organic material is deposited on the electrode are studied. But there are also studies for inversed systems [10, 15].

Although UPS is a widely used method, its use in the studies of organic materials is related to several problems. During the measurements, the electrons are emitted from the molecules close to the surface. The created holes need to be filled with electrons to avoid surface charging which leads to the effects like: 1) decrease of the signal due to the decrease of the number of molecules which can emit electrons; 2) increased Coulombic attraction (decreased kinetic energy of electrons) which leads to incorrect results. Due to the low charge carrier mobility, the studied organic material films are usually only a couple of tens of nm thick. As it is shown by N. Koch et al., the surface charging can be diminished if the sample is irradiated by the laser during the measurements [16]. It is explained by the photoconductivity which helps to fill the holes near the sample surface.

The problems can be caused by the ultraviolet (UV) radiation itself. It has been shown that the UV induced degradation of organic materials can alter the UPS spectrum [16–18].

2.2 Organic compound – organic compound system studies using UPS

In the devices made of organic materials, the active layer often consists of two compounds. There are two possibilities: either planar heterojunction is made or organic compounds are mixed together. Nevertheless, there is not a lot of research done concerning organic compound – organic compound (OC-OC) interface and its influence on the energy levels of the materials. Most of such

studies are done for a planar system where one material is deposited on top of the other and ionization energy dependence on film thickness is studied. I. G. Hill et al. have studied energy levels at different OC-OC interfaces [19]. The obtained results showed that only in some cases the vacuum level shift can be observed. In most of the cases, no vacuum level shift at the OC-OC interface was observed or it was within the precision of the measurements (0.1 eV). It is being explained by the properties of organic materials: as the electrical conductivity is relatively low and charge carriers are strongly localized on the molecules, electron transport from one material to other is limited. This is why interface dipole formation and vacuum level shift due to the redistribution of charge carriers is limited.

Nevertheless, Gao et al. have observed vacuum level shift and so-called band bending at the OC-OC interface, when studying materials for organic thin film transistors [20]. As the organic material films for UPS measurements are very thin (only couple of tens of nm), there have been observed energy level shifts at the OC-OC interface which are influenced by the electrode beneath the organic material film [21, 22].

Although most of the research concerning OC-OC interface is done for systems obtained by the thermal evaporation in a vacuum, there are studies where samples are made from solutions. One of such studies is related to the polymer poly(3-hexylthiophene-2,5-diyl) (P3HT) energy level shift near the interface with poly(3,4-ethylene dioxythiophene):poly(styrene sulfonate) (PEDOT:PSS) [23]. Such studies are hindered by the fact that during the production of the samples the solvent for the upper layer can dissolve the bottom layer, creating a mixture of compounds instead of separate layers.

The active layer of OPV cells usually consists of the mixture of two compounds – electron donor and an electron acceptor material. To obtain correct results, the energy level and their shift measurements should be done in mixed systems. E. L. Ratcliff et al. have shown that there are significant differences between energy levels obtained for pure compounds and energy levels in the mixed film [24]. It shows that the energy level values obtained for neat films of separate materials can give false expectations about their performance in real systems. Huai-Xin Wei et al. have studied the sample treatment (annealing in different temperatures) influence on the energy levels [25]. The annealing of the sample leads to the phase separation and alignment of the molecules, which leads to the vacuum level shift due to the interface dipole. Chi Yan has shown the energy level shifts depending on the mass ratio of the compounds in the film [26].

One of the most popular bulk heterojunction systems for OPV cells is a mixture of polymer P3HT and fullerene derivative [6,6]-Phenyl-C_{61}-butyric acid methyl ester (PCBM). In the studies, P3HT:PCBM mass ratio gradient has been observed: P3HT concentration near the sample surface is higher than that of PCBM due to the lower surface energy [27]. As the scanning depth of UPS

is only up to 2 nm, no signal created by PCBM could be observed in the study done by Ze-Lei Guan. Because of that, the film was lifted off of the substrate and the previously hidden surface was studied [28]. In this case, the electrode influence was observed: the results were different for the sample made on a pure silicon wafer or on the gold which was deposited on a silicon wafer. There has been performed the research related to the energy level values depending on P3HT:PCBM mass ratio [29]. Again, the obtained signal was mostly created by the polymer, which fundamentally hinders the studies of mixed systems. W. C. Tsoi et al. have studied P3HT:PCBM energy level shifts caused by the P3HT itself – whether the monomers of P3HT are ordered (regioregular P3HT – RR-P3HT) or not (regiorandom P3HT – RRa-P3HT) [30]. Authors obtained that in the case of RRa-P3HT the ionization energy was 0.3 eV higher than that of RR-P3HT. In the P3HT:PCBM systems the influence of PCBM was negligible and energy level shifts were within 0.08 eV which coincides with the precision of the measurement. After the annealing of the samples, the influence of PCBM disappeared almost completely and the obtained UPS spectra of P3HT:PCBM systems were almost identical to those of pure P3HT layers. This again is explained by the low concentration of PCBM near the surface of the sample and small scanning depth of UPS.

2.3 Molecule ionization energy determination using PYS

Photoelectron yield spectroscopy can be used for molecule ionization energy determination as an alternative to the UPS. Although this method is not so common, it has some advantages.

Contrary to the UPS where measurements are carried out in ultra-high vacuum (UHV), PYS measurements can be carried out in the air [31–35]. In this way work function of several metals has been determined [36], as well as in the combination with scanning Kelvin probe the perovskite materials in Solar cells are studied [37]. Even more, using PYS it is possible to study the influence of different gases on the organic materials and their energy levels [38].

PYS allows to obtain ionization energy of materials as well as to study the energy level shifts near the metal – organic compound interface. Similarly to the UPS, a film of organic material using thermal evaporation in a vacuum is deposited on the electrode, thus obtaining energy level shift at the metal – organic compound interface. In such measurements, the gold work function decrease of almost 1 eV was observed when pentacene thin film was deposited. The obtained shift is explained by the formation of interface dipole. A similar shift of 0.80 eV was observed when gold was covered with copper phthalocyanine thin film. [39]

Thus far, the PYS has rarely been used in the studies of OC-OC interface, so this topic has not been widely discussed. As an example, PYS has been used in

the metal-organic compound (gold (Au)/ rubrene) and OC-OC (Au/ rubrene/ C_{60}) system studies [40].

To our best knowledge, there are no studies related to the mixture of two organic compounds using PYS.

2.4 Scanning Kelvin probe

Scanning Kelvin probe (SKP) is a simple method for metal work function determination. It can be used for determination of work function changes, for example, indium tin oxide (ITO) work function shift caused by the UV radiation [41, 42].

In some cases, SKP is successfully applied in the studies of organic materials, for example, in the studies of metal and polymer interaction [43], as well as in the determination of Fermi level values in perovskite solar cells [37]. In the latter case, by combining SKP and photoelectron emission it was possible to observe the energy level alignment and shifts at the interfaces between different materials. N.Hayashi et al. have shown that metal work function has no influence on the C_{60} surface potential in the metal/C_{60} systems [44]. Similar results were obtained by T. R. Ohnoet al., who have studied metal/C_{60} interfaces using UPS [45]. Authors conclude that in these cases the obtained results describe the Fermi energy level of C_{60}.

The opposite situation was obtained by E. Kinbaraet al., who studied poly(3-arylthiophene) derivatives and their interfaces with metals. In some cases, the obtained surface potential was directly proportional to the work function of the metal beneath the thin film [46]. Similar results were obtained by Y. Harima et al., who studied different organic compounds [47]. The authors explain these results by the low charge carrier transfer at the metal / organic compound interface caused by the blocking layer on the surface of the metal, instead of the properties of organic materials. By measuring the diffusion potential and applying Schottky-Mott rule [48], the authors could diminish the influence of the metal work function on the surface potential in the case of several phthalocyanines. Yet, in other cases, there was a considerable difference between the surface potential values obtained by SKP and values obtained by diffusion potential measurements and Schottky-Mott rule. These differences are explained by the oxygen and water created surface states which influence the SKP measurements.

There has been observed surface potential dependence on metal work function for metal/ N,N′-Bis(3-methyl phenyl)-N,N′-diphenyl benzidine (TPD) thin films [49, 50]. Authors offer two possible explanations for this effect: 1) the metal / TPD system is in thermodynamic equilibrium and the Fermi levels of metal and TPD align, but the obtained surface potential describes all the system, instead of organic material alone; 2) system is not in thermodynamic

equilibrium and there is no Fermi level alignment at the metal/ TPD interface due to the poor transfer of charge carriers [51].

Thus far the results obtained by SKP are as various as the possible explanations for these results. There still has not been done systematic research to show what properties of organic materials influence the obtained surface potential and its dependence on metal work function. Mostly, the results are explained in the "case by case" manner. Because of this, the SKP is mostly used in relative measurements, instead of using it in the Fermi level measurements in organic materials. For example, SKP is widely used in the research related to the gas diffusion in materials [52, 53], as well as in the studies of various alloys and their corrosion [54–56].

3 EXPERIMENTAL PART

3.1 Methods for the production of the samples

3.1.1 Wet casting method

Most of the organic thin films were made from solutions using the spin-coating method. In this method, the substrate is initially covered with the solution of the organic compound. As the substrate rotates, most of the solution is thrown away due to the centripetal force. As the solvent evaporates, the viscosity of the solution increases until a solid and uniform thin film of the studied material is obtained.

In this work, a spin-coating system Laurell WS–650 Sx–GNPP/Lite was used. This equipment allows setting the rotation speed, the acceleration, and the duration of the rotation.

3.1.2 Thermal evaporation in vacuum

Thermal evaporation in a vacuum is based on the evaporation of solid materials at certain temperature and pressure, with the following deposition of material on the substrate. This method was used for the deposition of insoluble low molecular weight organic compounds as well as the deposition of metal electrodes.

The organic materials were deposited using self-made thermal evaporation system. This system consists of a vacuum chamber, a turbomolecular pump, a stand with sample holders, crucibles for evaporation, and a current source. Sublimation was done when the pressure in the vacuum chamber was $1 \cdot 10^{-5}$ mbar or lower.

Metal electrodes were deposited using Edwards Auto 306 thermal evaporation in a vacuum system. The evaporation of metals was done at the pressure of $1 \cdot 10^{-5}$ mbar. The deposition rate and thickness were controlled using calibrated quartz resonators.

3.1.3 Preparation of the substrates (etching of ITO)

A glass covered with ITO was used as a substrate in all the photoelectrical measurements. The resistivity of ITO was 20 Ω/sq. To obtain the desired shape and size of the electrode, it was necessary to etch away part of the ITO. Scotch Crystal tape was stuck on the 1 × 1 inch big substrates. Afterward, the substrates were immersed in hydrochloric acid and zinc pellets were added. In their chemical reaction, hydrogen was produced which etched away the bare ITO. Afterward, the substrates were rinsed with deionized water, the scotch tape was

removed, and substrates were rinsed with acetone. In the next step, the substrates were immersed in chloroform and ultrasonically cleaned for 15 min, which was followed by 15 min ultrasonic cleaning in acetone. This was followed by the rinsing with deionized water and 15 min long ultrasonic cleaning in 2 % detergent solution. After that, the substrates were again rinsed with deionized water and ultrasonically cleaned in deionized water for 15 min. In the end, the substrates were ultrasonically cleaned in isopropyl alcohol for 15 min.

3.2 Experimental methods and equipment

3.2.1 Ionization energy measurements

Samples for molecule ionization energy measurements were made on ITO covered glasses. By using the etching procedure described in chapter 3.1.3, 1 cm wide ITO electrode was made. The organic thin film was deposited by one of two methods – thermal evaporation in a vacuum of spin-coating.

Thin films were made from a chloroform solution. The concentration of the studied compound in the solution was 40 mg/ml. Spin-coating parameters were: rotation speed – 400 rpm, acceleration – 400 rpm/s, rotation time – 40 s. Afterward, the samples were dried on a hot plate at 70 °C for 15 min. The obtained samples were about 400–500 nm thick which allowed avoiding the influence of the electrode, as well as completely covered substrate, making the uniform film.

Insoluble organic compounds were deposited using thermal evaporation in vacuum. Samples were produced using a self-built thermal evaporation system. The evaporation was done at $1 \cdot 10^{-5}$ mbar or lower pressure with the rate of 0.5–1 nm/s.

In the sample series, where ionization energy dependence on film thickness was measured, this thickness was varied depending on the method used in the production of samples: in thermal evaporation, the thickness of the samples was varied by the evaporation time; in spin-coating the concentration of the solution was varied.

For molecule ionization energy measurements, a photoelectron yield spectroscopy system was built in the Laboratory of Organic Materials, Institute of Solid State Physics, University of Latvia. The setup of the system is shown in Fig. 3.1. PYS system consists of: 1) white light source (Energetiq LDLS EQ-99), 2) monochromator (MYM-1), 3) stepper motor, 4) stepper motor control unit, 5) shutter (Newport 76993), 6) cylindrical quartz lens, 7) valve, 8) valve, 9) turbomolecular vacuum pump (Ilmvac CDK 240), 10) vacuum pump (Edwards nXDS 6i), 11) electrometer (Keithley 617), 12) computer, 13) copper electrode for collection of emitted electrons, 14) sample holder with sample.

UV radiation was focused on a slit in the electrode. After passing the slit (2×15 mm) the beam expanded and irradiated 6×15 mm big surface area. As the electrons are emitted from the sample surface, the aim was to irradiate as big area as possible.

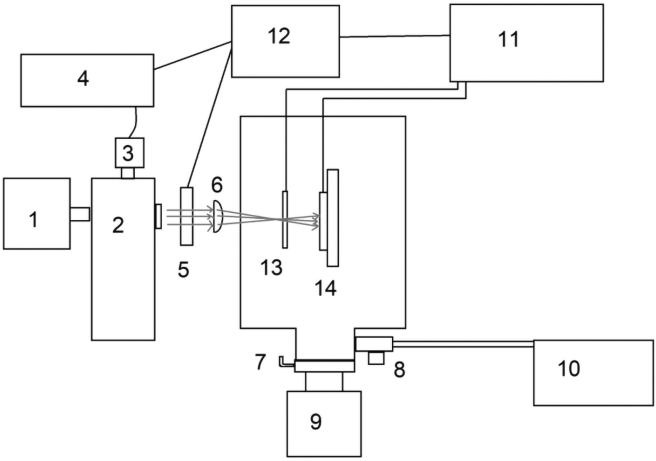

Fig. 3.1 **Scheme of PYS system. Numbers are explained in the text**

In this work, the software was made which allowed to automatize the measurements and to save all the data in MS Office Excel program.

UPS measurements were done in collaboration with the company Physical Electronics (USA), using PHI VersaProbe III multifunctional UPS/XPS scanning device. Samples were irradiated with 21.22 eV (He I line) monochromatic radiation. The angle between incident UV radiation and emitted electrons was 90°.

3.2.2 Photoconductivity measurements

In the photoconductivity measurements, the same samples as in ionization energy measurements were used. On the surface of these samples, using Edwards Auto 306 thermal evaporation system the aluminum (Al) electrodes were deposited. The deposition rate was between 0.15 and 0.20 nm/s and the thickness was 25 nm. At such thickness, Al has good electrical conductivity and is semitransparent (light transmission of around 40–50 %) which allowed to irradiate the sample through the electrode. In this way, the "sandwich" type samples (glass/ ITO/ studied compound/Al) were obtained.

The photoconductivity measurement system was similar to the PYS system. Instead of the copper electrode which was 2 cm away from the sample, the upper electrode was deposited directly on the surface of the sample. In this case, the electrical contacts were attached to the Al and ITO. In photoconductivity measurements, the light was focused on 3 × 3 mm big Al and ITO intersection area. The photoconductivity spectrum was obtained with the 5 nm step. The spectral range was chosen depending on the light absorption spectrum of the studied compound.

3.2.3 Surface potential measurements

Samples were made on glasses where ITO was etched leaving only 5 mm wide electrode. Afterward using Edwards Auto 306 thermal evaporation system the rest of electrodes – aluminum (Al), silver (Ag), gold (Au), and copper (Cu) – were deposited. The deposition was done at $1 \cdot 10^{-5}$ mbar or lower pressure with the rate of 0.15–0.20 nm/s. Each of the electrodes was around 5 mm wide with a 1 mm gap between the electrodes. The shape and placement of electrodes were controlled with shadow masks. Each sample had four different electrodes (see Fig. 3.2).

Thin films of such organic materials as 2-(4-[N,N-dimethylamino]-benzylidene)-indene-1,3-dione (DMABI), fullerene derivatives (C_{60}, PCBM, and [6,6]-Phenyl-C71-butyric acid methyl ester ($PC_{71}BM$)), (2,5-cyclohexadiene-1,4-diylidene)-dimalononitrile (TCNQ), and TPD were made by the thermal evaporation in vacuum using self-built system. With the help of shadow masks, it was possible to obtain samples where only half of the substrate was covered with studied material (see Fig. 3.2). It allowed measuring the work function of metal as well as the surface potential above each electrode.

The rest of the compounds – P3HT, poly(9-vinylcarbazole) (PVK), poly(methyl methacrylate) (PMMA), 2-(4-(bis(2-(trityloxy)ethyl) amino) benzylidene)-2H-indene-1,3-dione (DMABI-6Ph) – were dissolved in chloroform and samples were produced using spin-coating.

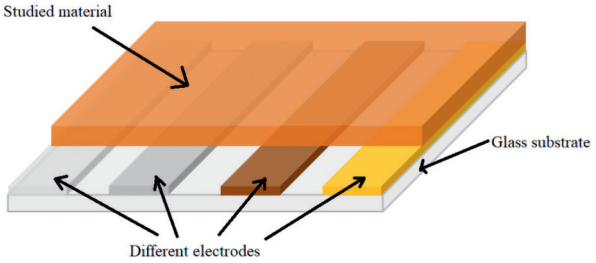

Fig. 3.2 **Scheme of the sample for surface potential measurements**

The samples were produced in the same way as described previously in chapter 3.2.1. The thickness of these samples was between 400 nm and 600 nm.

The surface potential of organic materials was measured using KP Technology SKP5050 Kelvin probe, which has a precision of 3 meV. Kelvin probes made by KP Technology use so-called "peak-to-peak" principle, where the applied voltage (U_{appl}) is varied in a wide range and the obtained voltage (U_{ptp}) is measured [57]:

$$\boldsymbol{U_{ptp} = \left(\Delta\Phi - U_{appl}\right) R C_0 \omega \epsilon \sin(\omega t + \theta)} \qquad 3.1$$

where $\Delta\Phi$ is the work function difference between the sample and the probe, R is the resistivity of I-V converter, C_0 is the average capacity of Kelvin probe, ϵ modulation index, ω is the angular frequency of vibration, and θ is the phase angle. As there is a linear relation between U_{appl} and U_{ptp}, $\Delta\Phi$ can be easily determined.

Prior to each series of measurements, SKP was calibrated using highly oriented pyrolytic graphite (HOPG) sample with known work function: Φ_{HOPG} = 4.93 ± 0.03 eV [47].

3.2.4 Absorption spectra measurements

Samples for light absorption measurements were made either on a slide glass or on quartz glass. Thermal evaporation in vacuum or spin-coating was used as a method for production of samples depending on the solubility of the organic compound. The thickness of these samples usually was between 100 nm and 150 nm.

To obtain such films, a solution with a concentration of 10 mg/ml was used. Spin-coating parameters were: rotation speed – 400 rpm, acceleration – 400 rpm/s, rotation time – 40 s. Afterward, the samples were dried on a hot plate at 70 °C for 15 min.

Most of the films obtained by thermal evaporation in vacuum were polycrystalline. It was not possible to obtain correct absorption spectra of such films due to the light scattering in the film. The samples of compounds which formed optically clear films were deposited at $1 \cdot 10^{-5}$ mbar or lower pressure with the rate of about 0.5 nm/s.

Light absorption spectra were measured with high-resolution spectrometer Ocean Optics HR4000CG-UV-NIR. Its range of measurement is between 200 nm and 1100 nm, but usually, the spectral range from 300 nm to 700 nm wavelength was used.

3.2.5 4-probe method for determination of electrical conductivity

Samples for the 4-probe method were made on a clean glass substrate. Initially, the organic material thin film was deposited either by thermal evaporation in a vacuum or by the spin-coating method. Afterward, the copper electrodes were deposited using Edwards Auto 306 thermal evaporation in a vacuum system. The placement and shape of electrodes were obtained using shadow masks. The parameters of sample productions were the same as described in chapter 3.2.1.

The scheme of the sample is shown in Fig. 3.3.

The system of 4-probe measurements consisted of KEITHLEY 6487 amperemeter with a built-in voltage source, and KEITHLEY 6514 electrometer. Electrometer was connected to the middle electrodes (see Fig. 3.3) and the voltage between these two contacts was measured. The amperemeter was connected to the outer electrodes. From the measured current-voltage characteristics and the parameters of the sample, the electrical conductivity of the material was calculated.

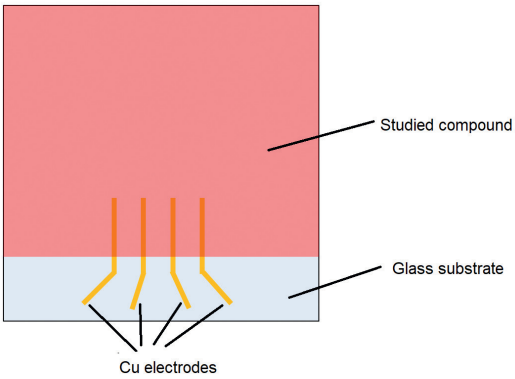

Fig. 3.3 **Scheme of the sample for electrical conductivity determination**

3.2.6 Film thickness measurements

The thickness of the studied thin films was measured using surface profiler Veeco Dektak 150. In this method, the position of the probe is constantly registered as it slides over the surface of the sample. As the organic materials are relatively soft, the force which is applied to the surface by the probe was chosen to be low (~ 10 μN). In this work, for all the measurements, the diameter of the probe tip was 12.5 μm.

3.2.7 Scanning electron microscope measurements

Tescan Lyra SEM-FIB scanning electron microscope was used as equipment for the sample morphology studies. The electrons accelerating voltage was between 5–10 kV. In this work, the magnification was between 1000 × and 10 000 ×.

3.2.8 Photovoltaic effect measurements

Samples for photovoltaic effect measurement were made on ITO covered glasses where ITO was etched leaving 1 cm wide electrode. At first, PEDOT:PSS film, which worked as a hole extraction layer, was obtained by spin-coating. The spin-coating parameters were: rotation speed – 2500 rpm, acceleration – 2500 rpm/s, rotation time – 80 s. Afterward, the samples were dried on a hot plate at 150 °C for 30 min. the thickness of PEDOT:PSS layer was about 40 nm.

The active layer was made by mixing studied compound (one of the three pyranylidene fragment containing compounds) and PCBM in the chloroform solution. The mass ratio was 1:1 and the concentration of the solution was 60 mg/ml. The active layer was deposited by spin-coating with parameters: rotation speed – 300 rpm, acceleration – 300 rpm/s, rotation time – 40 s. Afterward, the samples were dried on a hot plate at 120 °C for 15 min.

The electrodes were deposited using Edwards Auto 306 thermal evaporation in a vacuum system. At first, 1nm thick barium fluoride (BaF_2) layer was deposited with a rate of 0.06 nm/s. BaF_2 in this system worked as an electron extraction layer. On top of BaF_2, the 80 nm thick Al electrodes were deposited. The shape and placement of BaF_2 and Al were controlled with the help of shadow masks.

The obtained sample structure was ITO/ PEDOT:PSS/ studied compound: PCBM/BaF_2/Al.

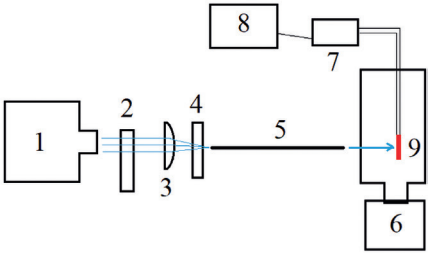

Fig. 3.4 **Setup for photovoltaic effect measurements. Numbers are explained in the text**

The parameters which characterize photovoltaic effect were obtained from current-voltage characteristics measurements, where the voltage was varied from –0.10 V to (U_{oc} + 0.04) V with the step of 0.01 V. In the experiments the system shown in Fig. 3.4 was used. It consisted of: 1) xenon lamp as a light source, 2) filter holder with interference filters (Andover Corporation), 3) quartz lens, 4) shutter (Newport 76993), 5) optical fiber, 6) turbomolecular pump (Ilmvac CDK 250), 7) electrometer (KEITHLEY 6517B), 8) computer, 9) vacuum chamber.

The measurements were done in a vacuum (pressure of $1 \cdot 10^{-5}$ mbar) to avoid the influence of the oxygen and moisture.

4 RESULTS AND DISCUSSION

4.1 Photoelectrical measurements of pyranilidene fragment containing compounds

For this research, three original compounds who contain 2-tert-butyl-6-methyl-4H-pyran-4-ylidene group were chosen: 2-(2-tert-Butyl-6-methyl-4H-pyran-4-ylidene)-1H-indene-1,3(2H)-dione (ZWK-1TB), 5-(2-tert-Butyl-6-methyl-4H-pyran-4-ylidene)pyrimidine-2,4,6(1H,3H,5H)-trione (JWK-1TB), 2-(2-tert-Butyl-6-methyl-4H-pyran-4-ylidene)malononitrile (DWK-1TB). The molecules of the studied compounds are shown in Fig. 4.1.

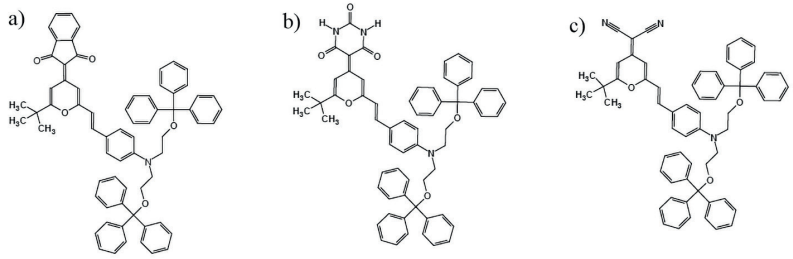

Fig. 4.1 **Chemical structure of the studied compounds a) ZWK-1TB, b) JWK-1TB, c) DWK-1TB. Full names are given in the text**

The bulky trityloxyethyl groups in the investigated compounds attached to the electron acceptor group diminish the interaction between molecules and help in the formation of amorphous films from solutions. The synthesis of these compounds is described in [58]. The absorption of these materials is in the spectral range between 400 nm and 600 nm and is close to the spectrum of the Sun. It could allow obtaining highly efficient OPV cells.

4.1.1 Energy level determination

The ionization energy of the studied compounds was determined by PYS. In Fig. 4.2 a, the photoelectron yield spectral dependence of DWK-1TB sample is shown. This spectrum is extrapolated to $Y^{2/5}(h\nu) = 0$. The obtained point is considered to the the ionization energy of the material.

For the studied compounds, the photoconductivity measurements were done to obtain the value of the energy gap between ionization energy and electron affinity. From these measurements the quantum efficiency of photoconductivity

and its spectral dependence ($\beta(h\nu)$) was obtained. The point where $\beta^{2/5}(h\nu) = 0$ was found (see Fig. 4.2 b). This is considered to be the photoconductivity threshold energy (E_{th}) [59, 60].

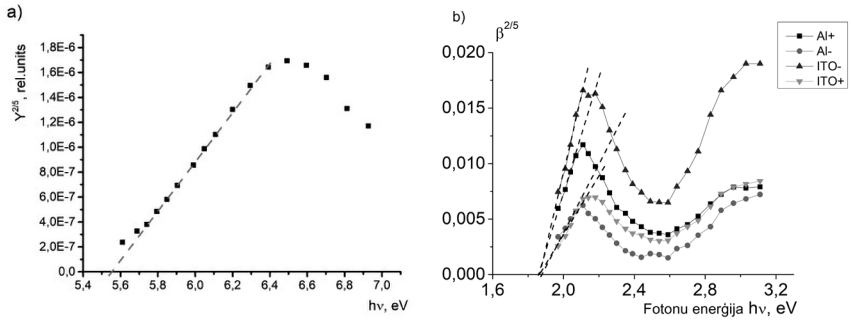

Fig. 4.2 **a) Ionization energy determination of DWK-1TB; b) JWK-1TB photoconductivity threshold energy determination**

The electron affinity (E_a) of the studied materials was calculated as a difference between ionization energy (I) and photoconductivity threshold energy (E_{th}):

$$E_a = I - E_{th} \tag{4.1}$$

Similarly, the energy levels of electron acceptor material PCBM was obtained. The energy level values of these materials are collected in Table 4.1.

Table 4.1 **The energy level values of pyranilidene fragment containing compounds and the theoretical open circuit voltage value in the "studied compound: PCBM" Solar cell**

Organic compound	I, eV (± 0.03 eV)	E_{th}, eV (± 0.03 eV)	E_a, eV (± 0.05 eV)	U_{oc}, V (± 0.08 V)
DWK-1TB	5.56	1.98	3.58	1.63
JWK-1TB	5.42	1.86	3.56	1.49
ZWK-1TB	5.49	1.68	3.81	1.56
PCBM	6.08	2.45	3.63	

Open circuit voltage (U_{oc}) shows the maximum voltage that can be obtained from the OPV cell. U_{oc} can be calculated from the empirical equation:

$$U_{oc} = \frac{1}{e}\left(I_d - E_{a,a}\right) - 0,3V \tag{4.2}$$

where I_d is ionization energy of electron donor material and $E_{a,a}$ is the electron affinity of the electron acceptor material, e is elementary charge [61]. From the obtained results, the U_{oc} for each studied material in combination with PCBM was calculated (see Table 4.1). The expected values are high, as the U_{oc} in OPV cells is usually only up to 1 V [62].

4.1.2 Photovoltaic effect measurements

Spectral dependence of current-voltage characteristics was measured for the "studied compound: PCBM" systems. The obtained characteristics show distinct differences between JWK-1TB:PCBM (Fig. 4.3 a) and ZWK-1TB:PCBM (Fig. 4.3 b) samples.

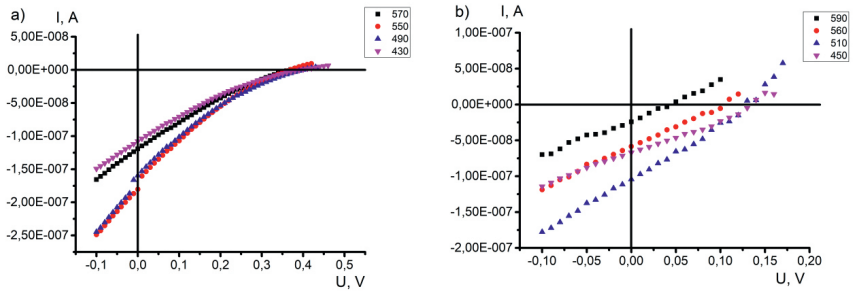

Fig. 4.3 **Examples of current-voltage characteristics for a) JWK-1TB:PCBM and b) ZWK-1TB:PCBM samples at the various wavelengths**

While the short-circuit current (i_{SC}) is similar in both cases (~ $1 \cdot 10^{-7}$ A), the obtained U_{oc} value for JWK-1TB:PCBM is 0.40 V and only 0.17 V for ZWK-1TB:PCBM sample, while the expected value was around 1.50 V. Also, the curve in the case of JWK-1TB:PCBM is concave, which indicates that there are problems with charge carrier extraction from the sample.

From the measured current-voltage characteristic the parameters which characterize the photovoltaic effect – the density of short-circuit current j_{sc} (μA/cm²), open circuit voltage U_{oc} (V), and Incident Photon to Charge Carrier Efficiency IPCE (%) – were obtained. IPCE % can be calculated as:

$$\boldsymbol{IPCE}(\%) = \frac{\boldsymbol{j_{SC}(mA/cm^2)}}{\boldsymbol{i_{kr}(mW/cm^2)}} \cdot \frac{\boldsymbol{1240}}{\boldsymbol{\lambda(nm)}} \cdot \boldsymbol{100} \qquad 4.3$$

where i_{kr} is the intensity of the incident light [63]. The spectral dependence of IPCE shows the spectral region where OPV cell works efficiently and where heavy losses are [64]. The obtained results are collected in Table 4.2.

Table 4.2 The maximum values of photovoltaic effect describing parameters

System	$j_{sc,max}$, μA/cm^2	$U_{oc,max}$, V	$IPCE_{max}$, %
ZWK-1TB:PCBM	0.76	0.17	0.3
JWK-1TB:PCBM	1.10	0.40	0.4
DWK-1TB:PCBM	2.50	0.60	1.0

In Fig. 4.4 a-c IPCE spectra of "studied compound:PCBM" systems is shown. In the cases of DWK-1TB:PCBM and JWK-1TB:PCBM a rapid decrease of IPCE near the absorption maximum of the studied compounds. It indicates that there are problems with the charge carrier extraction from these systems. In these samples, electrons and holes recombine before they can be extracted. The IPCE spectrum of ZWK-1TB:PCBM sample follows the absorption spectrum of ZWK-1TB, which shows that this system is the best in charge carrier extraction. Nevertheless, the IPCE of DWK-1TB:PCBM in its minimum is at least twice as efficient as ZWK-1TB:PCBM system in its best.

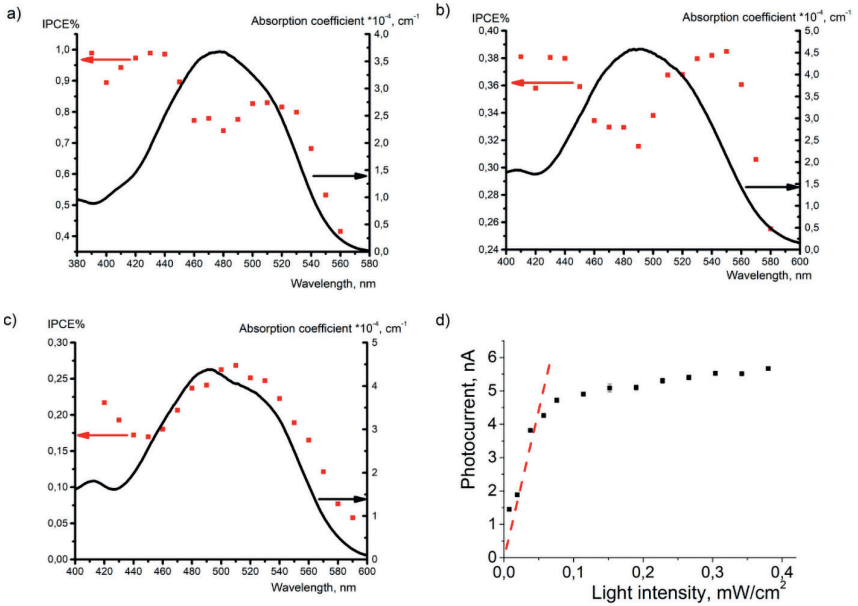

Fig. 4.4 **IPCE % and the absorption spectra of a) DWK-1TB:PCBM; b) JWK-1TB:PCBM; c) ZWK-1TB:PCBM sample; d) photocurrent dependence on light intensity at 490 nm wavelength for JWK-1TB:PCBM sample**

For the JWK-1TB:PCBM sample the photocurrent dependence on light intensity was measured. The wavelength was 490 nm as it corresponds to the maximum of the JWK absorption. As can be seen in Fig. 4.4 d, initially the photocurrent linearly increases with the increase of light intensity. But, as the light intensity reaches 50 μW/cm^2, the photocurrent rapidly saturates. It shows that only a small fraction of the generated charge carriers can be extracted from the JWK-1TB:PCBM system.

All the energy level measurements were done for relatively thick (400–500 nm) films but in the system layers with the thickness of less than 100 nm were used. It means that the energy level alignment at the of the metal-organic compound or OC-OC interfaces was not taken into account. It is possible, that here at one or both electrodes a blocking layer has formed, which hinders the charge carrier extraction from the sample.

4.1.3 Conclusions

Although from the obtained energy level values the open circuit voltage was expected to be around 1.50 V, 0.60 V was obtained in the case of DWK-1TB:PCBM and only 0.17 V in the case of ZWK-1TB:PCBM.

The rapid decrease of IPCE near the absorption maximum of JWK-1TB:PCBM system indicates that there are problems with charge carrier extraction from the system. It is confirmed by the photocurrent dependence on the light intensity measurements, which show that already at the light intensity of 50 μW/cm^2, the photocurrent value saturates.

Energy level values obtained from pure, thick films not always can show what the compatibility of materials will be in real systems. Studies showing the influence of the interfaces on the performance of the system are required.

4.2 Studies of the electrode-organic compound interface

The performance of such devices as OPV cells and OLEDs will be determined not only by the efficiency of each separate material but by the compatibility between these materials. That is why it is crucial to study the energy level (ionization energy and electron affinity) shifts near the interfaces between materials.

In this work two series of samples were made: in one series DMABI was deposited on the ITO covered glasses using thermal evaporation in a vacuum; in other series, DMABI-6Ph thin films obtained by spin-coating were studied. Photoelectrical properties of these compounds have been studied previously [65, 66].

DMABI (Fig. 4.5 a) forms polycrystalline thin films. To decrease the interaction between the molecules, both methyl groups in DMABI molecule were substituted by the bulky trityloxyethyl groups (Fig. 4.5 b). The added bulky groups help to form the amorphous films from solutions. Both of these compounds were synthesized in Prof. V. Kokars group at Riga Technical University. Synthesis of DMABI and DMABI-6Ph is described in [67, 68].

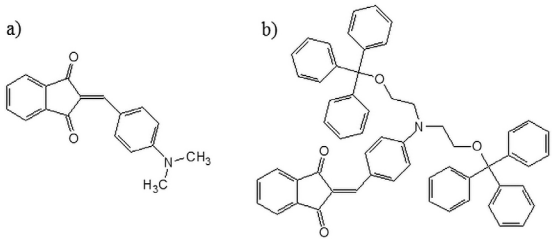

Fig. 4.5 **Studied compounds: a) DMABI; b) DMABI-6Ph**

To evaluate the quality and morphology of the films, images of the sample surface were obtained using a scanning electron microscope (SEM).

As no crystallites were observed in the case of DMABI-6Ph (Fig. 4.6 a-c), we can assume that the obtained films are amorphous. Without changing the spin-coating parameters, the film thickness can be varied by changing the compound concentration in the solution [69]. The lower is the concentration, the thinner films can be obtained. For the sample made out of solution with a concentration of 0.5 mg/ml only separate droplets of DMABI-6Ph could be observed

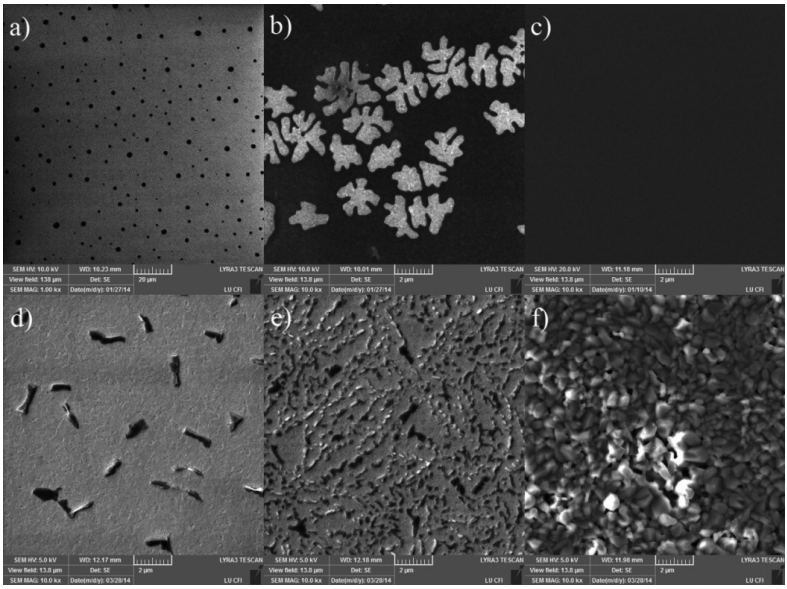

Fig. 4.6 **SEM images of the DMABI-6Ph films with thickness: a) 5 nm, 1000 × magnification; b) 20 nm, 10000 × magnification; c) 550 nm, 10000 × magnification; DMABI films with thickness: d) 20 nm, 10000 × magnification; e) 120 nm, 10000 × magnification; and f) 1500 nm, 10000 × magnification**

(dark spots in Fig. 4.6 a). By increasing the concentration of the solution, the size of these droplets increased and they started to combine, leaving only separate uncovered areas of ITO (light spots in Fig. 4.6 b). Uniform films were obtained from solutions with a concentration of 15 mg/ml or more. In that case, the DMABI-6Ph film thickness was 100 nm.

In the case of DMABI, the samples were polycrystalline. In the extreme case, only separate crystallites (Fig. 4.6 d) with the length between 500 nm and 1.5 μm were obtained. Even when the film thickness was 120 nm, the substrate was covered with separate crystallites, which started to form chain-like structures on ITO (Fig. 4.6 e). At the thickness of 1 μm, the ITO was fully covered and the uniform film was obtained (Fig. 4.6 f).

To obtain the work function of ITO, the dependence of $Y^{1/2}(h\nu)$ on the photon energy was plotted. The linear part of this graph was extrapolated till $Y^{1/2}(h\nu) = 0$, which is considered to be the work function of ITO. The obtained value was $\Phi_{ITO} = 4.79 \pm 0.03$ eV which is in good agreement with the values found in the literature [70, 71]. When ITO was covered with a thin film of an organic compound, its work function shifted, which is related to the vacuum level shift at the metal-organic compound interface. In the case of DMABI, the ITO work function increased by $\Delta = 0.40$ eV, reaching 5.20 eV (Fig. 4.7 a). Similar shift of work function was observed when ITO was covered with DMABI-6Ph. In that case, the shift was smaller ($\Delta = 0.30$ eV) and ITO work function reached 5.10 eV (Fig. 4.7 c). It is considered that such a vacuum level shift is caused by the electric dipole at the metal-organic compound interface [12, 13]. In this case, it could be caused by the alignment of permanent dipoles of the molecules at the ITO/ organic compound interface.

Ionization energy dependence on film thickness was obtained for both series of the samples. Fig. 4.7 a and c shows that after a linear increase of ITO signal there is rapid signal increase coming from organic materials. In that case, the photoemission yield can be expressed as a sum of two independent signals [72]:

$$\boldsymbol{Y(h\nu) = x(h\nu - \Phi_{ITO})^2 H(h\nu - \Phi_{ITO}) + y(h\nu - I)^{5/2} H(h\nu - I)} \qquad 4.4$$

where x and y are constants, showing the intensity of signal created by the ITO and an organic compound, respectively, H(E) is Heaviside step function, whose value is

$$\boldsymbol{H(E) = \begin{cases} 0, ja\ E \leq 0 \\ 1, ja\ E > 0 \end{cases}} \qquad 4.5$$

To obtain the ionization energy of the organic compounds, the signal created by ITO was subtracted, photoelectron yield $Y^{2/5}(h\nu)$ was plotted and again the linear part of the graph was extrapolated till $Y^{2/5}(h\nu) = 0$.

Fig. 4.7 b and d show photoelectron emission yield spectral dependence of DMABI and DMABI-6Ph samples with different thickness, respectively.

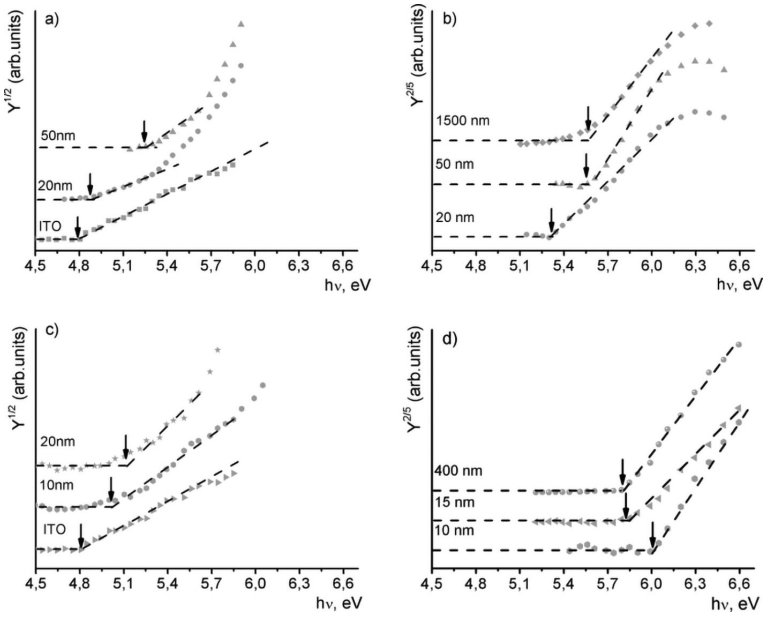

Fig. 4.7 **Work function and ionization energy determination depending on the organic layer thickness of a) ITO covered with a thin layer of DMABI; b) DMABI; c) ITO covered with a thin layer of DMABI-6Ph; and d) DMABI-6Ph**

In the case of DMABI, its ionization energy increase with the increase of film thickness. At the thickness of 70 nm, the ionization energy reached its plateau value of $I_{DMABI} = 5.55 \pm 0.03$ eV. Further film thickness increase did not change the ionization energy (see Fig. 4.8 a). In the case of DMABI-6Ph, the ionization energy decreased with the increase of film thickness. Here, the plateau value was obtained already at the thickness of 20 nm and was $I_{DMABI\text{-}6Ph} = 5.68 \pm 0.03$ eV (see Fig. 4.8 b).

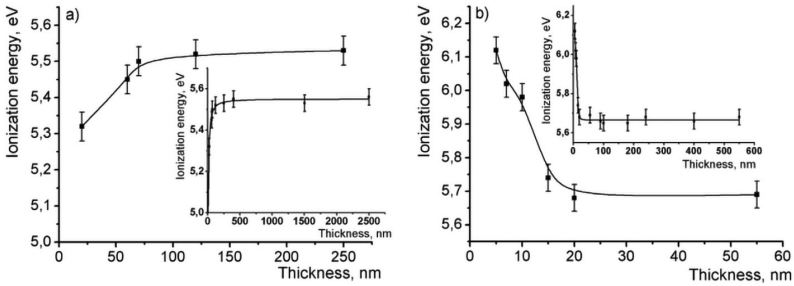

Fig. 4.8 **Ionization energy dependence on film thickness for a) DMABI; b) DMABI-6Ph. Insets show the full range of thickness**

All the energy level changes were observed for the samples with a thickness below 70 nm in the case of DMABI and below 20 nm in the case of DMABI-6Ph. As mentioned previously, continuous films were obtained only at around 1 μm for DMABI and 100 nm for DMABI-6Ph. It means that obtained energy level shifts are not related to the ITO coverage with an organic compound.

The energy gap between the ionization energy and electron affinity was obtained from photoconductivity measurements. In the case of DMABI, it was $E_{th,DMABI}$ = 1.91 ± 0.03 eV, but in the case of DMABI-6Ph-$E_{th,DMABI-6Ph}$ = 2.12 ± 0.03 eV. From the photoelectron emission and photoconductivity results the energy level scheme of DMABI and DMABI-6Ph can be proposed (see Fig. 4.9). At the ITO/DMABI interface the barrier for the electron transport from DMABI to ITO has formed, while at the ITO/DMABI-6Ph interface the barrier for hole transport has formed. Such differences with charge carrier blocking layers at the electrode/ organic compound interfaces is an essential aspect to take into account when creating devices (OPV cells or OLEDs) from organic materials.

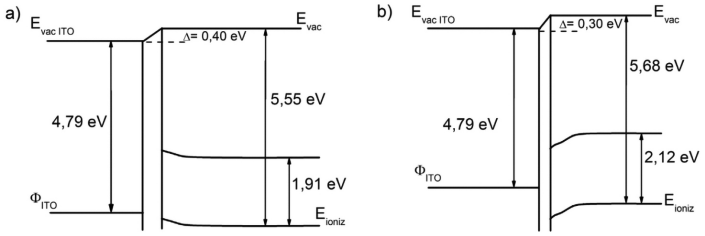

Fig. 4.9 **Energy level scheme of a) DMABI; b) DMABI-6Ph**

4.2.1 Conclusions

It was shown that PYS can be used in the metal / organic compound interface studies. Vacuum level shift at the ITO/organic compound interface as well as the ionization energy dependence on the organic material film thickness was observed. Additionally, taking into account the photoconductivity measurements, it was possible to construct the energy level scheme. Although the active part of the DMABI and DMABI-6Ph molecules is the same, the energy level shift at the interface with ITO was different: ITO/DMABI interface works as an electron blocking layer, while ITO/DMABI-6Ph blocks hole transport. Such information is crucial when multilayered devices are made.

SEM images showed problems related to the quality of thin films. First, both of the studied compounds tend to form separate islands instead of the uniform film at small thickness. In the case of DMABI-6Ph, a uniform film was obtained at the thickness of around 100 nm, while DMABI fully covered the surface of

the substrate only at 1 μm thickness. Second, film thickness measurements with surface profiler can give incorrect information. If the distance between separate islands is smaller than the tip of the probe, the obtained results can give a false impression of the uniform film, while the height of these islands is actually measured.

4.3 Studies of the organic compound–organic compound interface

The information about energy level shifts at the OC-OC interface is as important as knowledge about energy level shifts at the metal-organic compound interface.

4.3.1 Planar heterojunction

The ionization energy near organic compound–organic compound interface was studied for P3HT/PCBM system. Here, on top of the polymer P3HT film, a PCBM layer was deposited using thermal evaporation in vacuum. Fig. 4.10 a shows photoelectron emission yield spectral dependence for PCBM layers with various thicknesses. Two important things can be observed.

First, at small thickness of the upper layer, no signal coming from PCBM could be observed, while the P3HT signal amplitude decreased as the PCBM layer absorbed part of the UV radiation. Additionally, as the thickness of the PCBM layer increases, the scattering of electrons, coming from P3HT, also increases, which decreases the obtained signal.

Second, when the thickness of the PCBM layer reaches 15 nm, the photoelectron emission spectrum rapidly changes – signal created by P3HT cannot be seen anymore. It can be concluded that the scanning depth of PYS is between 12 nm and 15 nm. For comparison, the scanning depth of UPS is only 1.5–2 nm [12].

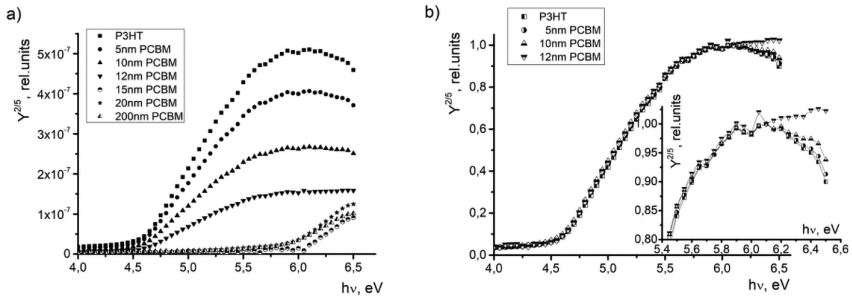

Fig. 4.10 **a) Photoelectron yield spectral dependence for all the samples; b) Normalized photoelectron yield spectral dependence. The inset shows high photon energy part of the spectra**

Photoelectron emission spectra, where P3HT signal can be observed, were normalized for easier comparison. As can be seen in Fig. 4.10 b, there are no P3HT ionization energy changes when PCBM layer thickness increases. Between 4 eV and 5.5 eV, these spectra are identical. It is possible that no energy level shift was observed because the number of molecules close to the OC-OC interface is negligible compared to the number of molecules in the bulk of the sample. In this case, the obtained molecule ionization energy of P3HT was $I_{P3HT} = 4.54 \pm 0.03$ eV. In the high photon energy end of the spectra, a small influence of PCBM can be seen (b and inset of it). For 5 nm and 10 nm thick films the UV absorption of PCBM is so small that the created signal is masked under the signal coming from P3HT. Upon reaching 12 nm film thickness, the PCBM signal has increased and can be observed in the high photon energy ($h\nu > 6$ eV) end of the spectrum (b and the inset).

To obtain the signal created by 12 nm thick PCBM layer, from the composite spectrum the P3HT signal was subtracted. The obtained spectrum is shown in Fig. 4.11 a. Upon reaching 15 nm, only the PCBM signal could be observed.

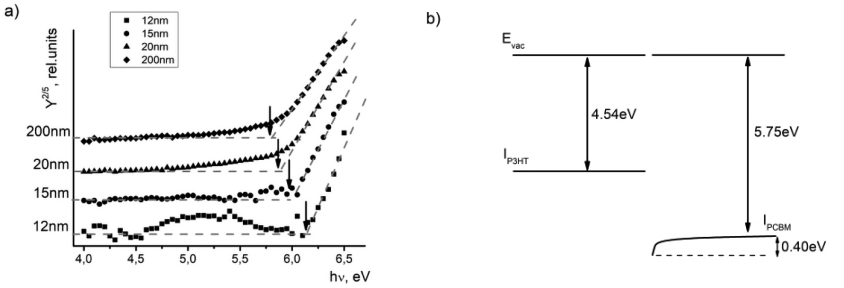

Fig. 4.11 **a) Normalized photoelectron yield spectral dependence of PCBM; b) Energy level scheme of P3HT/PCBM interface**

The most noticeable PCBM ionization energy shift can be observed in a narrow (around 20 nm) interface region. While the ionization energy for 12 nm layer was $I_{PCBM} = 6.15$ eV, in the case of 200 nm layer it reached around 5.75 eV. In this case, the P3HT/PCBM interface works as 0.40 eV barrier for hole transport from PCBM to P3HT. By collecting the results, energy level scheme for P3HT/PCBM interface can be proposed (see Fig. 4.11 b).

4.3.2 Bulk heterojunction

Surface morphology

As it was described in chapter 4.3.1, the small number of P3HT molecules near OC-OC interface compared to the number of molecules in the bulk of the sample could be the reason why no P3HT ionization energy level shift

was observed when PCBM layer was deposited on top of the film. Besides, in the OPV cells, the organic compounds are usually mixed together creating bulk heterojunction. In this way, the area of the interface is increased. This is why a system, where P3HT and PCBM are mixed together, was studied.

A pure P3HT sample made from a chlorobenzene solution was smooth. Adding the PCBM to the solution created changes in the morphology of the samples. As the portion of the PCBM in the sample increased, PCBM crystallites formed on the surface of the sample. When the P3HT:PCBM mass ratio was 1:3, the size of the PCBM crystallites was around 20 μm (Fig. 4.12 c). By increasing the portion of PCBM in the P3HT:PCBM mixture to 1:10, the crystallites covered even more of the sample surface and their size increased to 50–60 μm and created branch-like structures (see Fig. 4.12 d). Most likely, the sample preparation conditions like annealing temperature and time strongly influence the PCBM.

P3HT:PCBM samples made from chloroform solution were smooth and without any visible structures. Even when the P3HT:PCBM mass ratio was 1:10 and 1:50, no crystallites on the surface of the sample were observed (Fig. 4.12 b). The rapid evaporation of chloroform, as well as the relatively low annealing temperature (70 °C), precluded the aggregation of P3HT and PCBM.

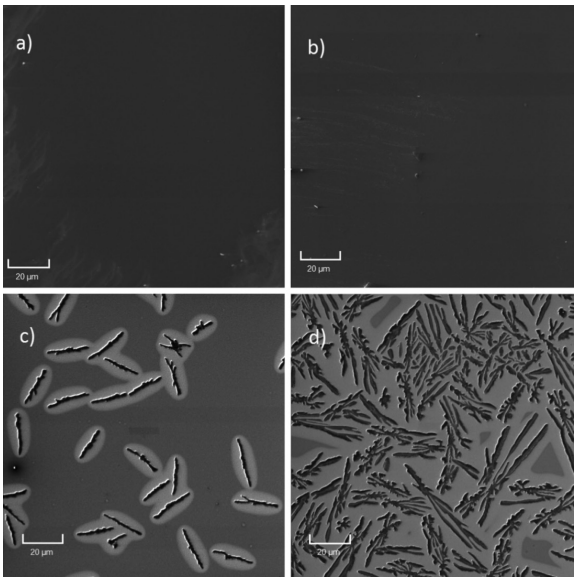

Fig. 4.12 **SEM images of a) P3HT sample made from the chloroform solution; b) P3HT:PCBM (1:10) sample made from the chloroform; c) P3HT:PCBM (1:3) sample made from the chlorobenzene solution; d) P3HT:PCBM (1:10) sample made from the chlorobenzene solution. Magnification in all the cases is 1000**

Ionization energy measurements for samples made from a chlorobenzene solution

For all the P3HT:PCBM samples made from chlorobenzene solution the photoelectron emission signal was obtained only from the polymer. PCBM influence in these measurements was negligible (Fig. 4.13). Even when the P3HT:PCBM mass ratio was 1:10, no signal coming from fullerene was observed. It can be explained by two effects. One, as can be seen in chapter 4.3.1, the signal created by PCBM is at least one order of magnitude lower than that of P3HT. Second, the ionization energy of PCBM is close to 6 eV, while P3HT ionization energy is 4.54 eV. It means that photons with the energy of about 6 eV ionize only small part of PCBM molecules, while P3HT molecules can be ionized easily. The combination of these two effects can mask the PCBM influence in the measured photoelectron emission signal. Here, in all the cases the obtained P3HT ionization energy was I_{P3HT} = 4.54 ± 0.03 eV which coincides with the value obtained for the bulky layer (see chapter 4.3.1).

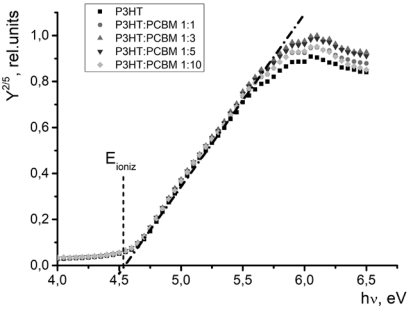

Fig. 4.13 **Photoemission yield spectra of bulk heterojunction samples depending on P3HT:PCBM mass ratio. Samples made from a chlorobenzene solution**

In these series of the samples, the signal is mainly obtained from the areas of pure P3HT, instead of molecules close to the OC-OC interface. It means that even samples with a high concentration of PCBM cannot be used in OC-OC interface studies if the aggregation of compounds occurs. It is because of the small portion of molecules close to the interface compared to the number of molecules in the bulk.

Ionization energy measurements for samples made from chloroform solution

The rapid evaporation of chloroform precludes the aggregation of P3HT and PCBM molecules, allowing obtaining a homogenous distribution of the compounds in the bulk of the sample. In OPV cells the generated exciton dissociation, as well as the charge carrier transfer from donor to acceptor molecules takes place at the OC-OC interface. This is why information about energy

levels of molecules at the interfaces is so crucial. By creating samples where organic compounds are homogeneously mixed in the bulk, the signal created by the molecules in the bulk of aggregates is diminished, but the properties of the molecules at the interface are not altered. In this case, the signal is obtained only from molecules near the OC-OC interface.

In the case of pure P3HT film, the obtained ionization energy was I_{P3HT} = 4.54 ± 0.03 eV and it was the same as obtained in our previous experiments. It shows that the chosen solvent does not influence the energy levels of pure film. By increasing the PCBM portion in the sample, the obtained photoelectron emission spectra shifted to higher energies (see Fig. 4.14). In the case of P3HT:PCBM mass ratio of 1:50, the P3HT ionization energy had increased by about 0.40 eV compared to the pure film and reached I_{P3HT} = 4.96 ± 0.03 eV. It means that near the OC-OC interface the difference between P3HT ionization energy and PCBM electron affinity increases. P3HT ionization energy dependence on P3HT:PCBM mass ratio is shown in the inset of Fig. 4.14. This kind of ionization energy shift could be explained either by the formation of interface dipole or the alignment of Fermi energy levels of the studied compounds. There are studies which show 0.50 eV vacuum level shift due to the P3HT:PCBM interface dipoles [28, 73]. Although it is in good agreement with the obtained 0.40 eV shift, it does not explain the relatively slow ionization energy shift depending on P3HT:PCBM mass ratio. This kind of ionization energy shift could be explained by the Fermi level alignment at the OC-OC interface. As the PCBM portion in the samples grows, the number of P3HT molecules near OC-OC interface increases as well. This situation is similar to the planar heterojunction where the thickness of the P3HT layer decreases. The closer the molecule will be to the interface, the more its energy levels will shift due to the Fermi level alignment. The further molecule will be from the interface, the closer its energy level values will be to those obtained for pure films.

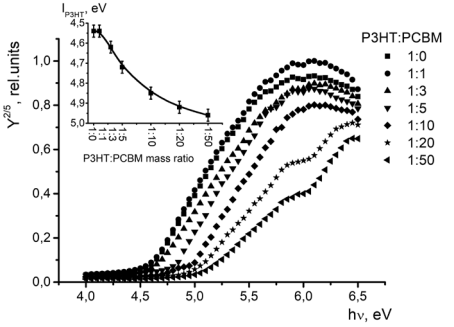

Fig. 4.14 **Photoemission yield spectra of bulk heterojunction samples made from chloroform solution depending on P3HT:PCBM mass ratio. Inset: P3HT ionization energy dependence on P3HT:PCBM mass ratio.**

The decrease of the signal amplitude, when the PCBM portion increases, is related to the decreased number of P3HT molecules in the studied film. The signal created by PCBM was observed only when the P3HT:PCBM concentration in the sample was 1:20 and 1:50. In both cases, the obtained PCBM ionization energy was I_{PCBM} = 6.15 ± 0.03 eV. It is the same value as in the case of 12 nm thick PCBM layer on top of the P3HT film, described in chapter 4.3.1. It means that despite the very high concentration of PCBM molecules in the film, the obtained electrons were coming from PCBM molecules close to the OC-OC interface.

UPS measurements for samples made from a chlorobenzene solution

In the collaboration with the company Physical Electronics (USA), UPS spectra were measured for samples made from chloroform solution. Here, the obtained P3HT ionization energy was $I_{P3HT,UPS}$ = 4.6 ± 0.1 eV, which is in good agreement with the values obtained by PYS. In this case no ionization energy shift depending on P3HT:PCBM mass ratio was observed (see Fig. 4.15). As can be seen in Fig. 4.15, for the samples with the P3HT:PCBM mass ratio of 1:3–1:50, as the PCBM portion in the sample, increases its signal increases as well. At the same time, the P3HT signal rapidly decreases. The PCBM ionization energy obtained by UPS was $I_{PCBM,UPS}$ = 5.9 ± 0.1 eV. The obtained ionization energy values for P3HT and PCBM correspond to the values obtained from pure films. This could be due to the low scanning depth of UPS in combination with less homogeneously distributed compounds at the surface of the sample.

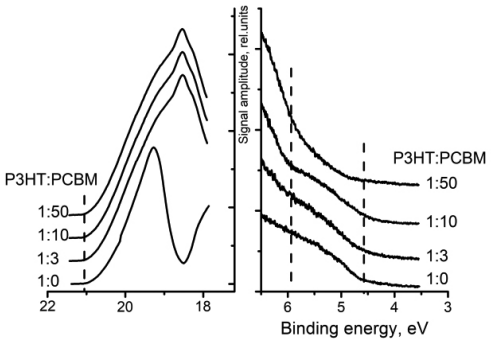

Fig. 4.15 **UPS spectra depending on P3HT:PCBM mass ratio showing secondary electron cutoff and low binding energy onset**

UPS spectra for samples with the P3HT:PCBM mass ratio of 1:3, 1:10 and 1:50 are nearly identical at the secondary electron cutoff end of the spectrum. Although there is a clear difference in the spectra between pure P3HT sample and the rest of the samples, no spectral shift was observed. The shift of

the secondary electron cutoff (high binding energy) is considered to be related to the vacuum level shift, due to the interface dipole. In this case, no shift was observed (see Fig. 4.15). It is in good agreement with the results obtained by PYS. The obtained energy level shift could be related to the Fermi level alignment of P3HT and PCBM, rather than vacuum level shift created by the interface dipole.

4.3.3 Conclusions

In the case of planar P3HT/PCBM samples, no ionization energy shift of P3HT was observed when PCBM layers with various thicknesses were deposited on top of the polymer film. No shift was observed due to the small number of molecules close to the interface, compared to the number of molecules in the bulk of scanned the sample.

It was determined that the scanning depth of PYS method is between 12 nm and 15 nm.

PCBM ionization energy dependence on film thickness was observed. In the case of thickest (200 nm) layer, the ionization energy was 5.75 eV, but near the interface with P3HT, it increased till 6.15 eV. The obtained 0.40 eV shift works as a barrier for hole transport from PCBM.

In the case of bulk heterojunction P3HT:PCBM samples, to make successful PYS measurements, the homogenous distribution of molecules in the bulk of the sample was required, to obtain as many molecules close to OC-OC interface as possible.

As the portion of P3HT in the film decreased, its ionization energy shift was observed. For pure P3HT film, it was 4.54 eV, but when P3HT:PCBM mass ratio was 1:50, the P3HT ionization energy reached 4.96 eV.

No ionization energy shifts were observed in the UPS measurements of P3HT:PCBM samples. The obtained values were the same as obtained from pure films of separate compounds.

4.4 Surface potential measurements

At first, using SKP the surface potential of all the electrodes was measured. From that, the work function (WF) of each electrode was obtained. The obtained values were: Φ_{Al} = 3.80 eV, Φ_{Ag} = 4.28 eV, Φ_{ITO} = 4.78 eV, Φ_{Cu} = 4.83 eV, Φ_{Au} = 4.95 eV. Between different sample series, the work function of the electrodes was stable within the precision of the experiment (± 0.03 eV). WF values obtained in this work using SKP were in good agreement with the values found in the literature [74].

Next, the surface potential of studied materials above each of the four electrodes was measured. In this way, the surface potential dependence on the metal work function for each studied material was obtained (see Fig. 4.16 a). In the case of metal (Al) the obtained surface potential did not depend on the metal electrode beneath it. On the other hand, in the case of PMMA, the obtained surface

potential was proportional to the metal work function, having a constant difference between the surface potential and the work. Based on the results, slope coefficient (S) can be introduced, which describes the relation between surface potential and metal work function [50, 51]:

$$S = \frac{d\Phi_{par}}{d\Phi_{met}} \tag{4.6}$$

It shows the changes in surface potential ($d\Phi_{par}$) depending on the changes in metal work function ($d\Phi_{met}$). If S = 0, the surface potential of the material does not depend on the metal, that is beneath it. This is the case of Al. If S = 1, then there is a direct correlation between material surface potential and metal work function (cases of PMMA and DMABI-6Ph). It means that materials with poor electrical conductivity and insulators work as the modificators of the metal surface. For organic semiconductors S was between 0 and 1, depending on the studied material. Generally, surface potential can be written as

$$\Phi_{par} = S \cdot \Phi_{met} + C \tag{4.7}$$

where C is a constant, depending on studied material.

As S = 0 for Al, S = 1 for dialectical material, and 0 < S < 1 for semiconductors, the one parameter which affects the slope coefficient could be the electrical conductivity of the studied material. Using the 4-probe method, the electrical conductivity for all the studied materials was measured. In Fig. 4.16 b, the relation between the slope coefficient and the electrical conductivity of studied materials is shown. As the electrical conductivity increases, the surface potential dependence on electrode work function decreases.

As the film thickness was not identical for all the samples, additional measurements were done (selected materials are shown as round dots in Fig. 4.16 b). Samples with various thicknesses were made for the chosen materials.

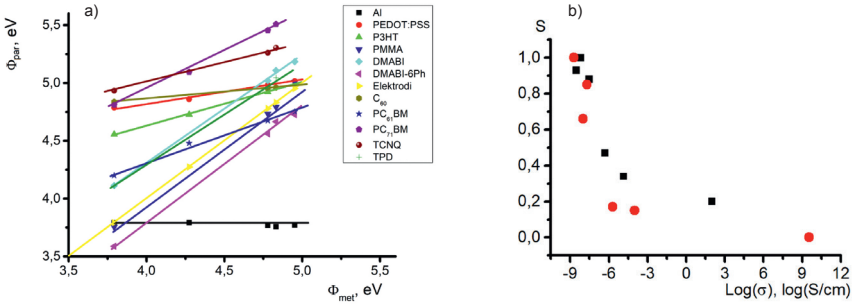

Fig. 4.16 **a) Surface potential dependence on metal work function for studied materials; b) Slope coefficient dependence on the electrical conductivity of the materials. Dashed lines are guides for eyes**

No metal work function influence on the Al work function was observed (Fig. 4.17 a). Although there are small differences in Al work function depending on film thickness, the results fit within the limits of measurements precision. On the other hand, as can be seen in Fig. 4.17 b and c, in the case of PMMA the obtained surface potential depends not only on the metal work function but also on the film thickness. As the film thickness increases, the difference between Φ_{PMMA} and metal work function increases as well, while the slope coefficient stays the same and is S = 1. Here, the surface potential can be written as:

$$\boldsymbol{\Phi_{PMMA} = \Phi_{met} + C(d)} \qquad 4.8$$

where C(d) is thickness-dependent constant.

In Fig. 4.17 c PMMA surface potential dependence on film thickness in the case of different electrodes is shown. Here, the surface potential is inversely proportional to the film thickness and directly proportional to the capacitance of the sample (C_S):

$$\boldsymbol{\Phi_{PMMA} = \Phi_{met} + A_d \frac{1}{d} = \Phi_{met} + B_d C_S} \qquad 4.9$$

where A_d and B_d are constants.

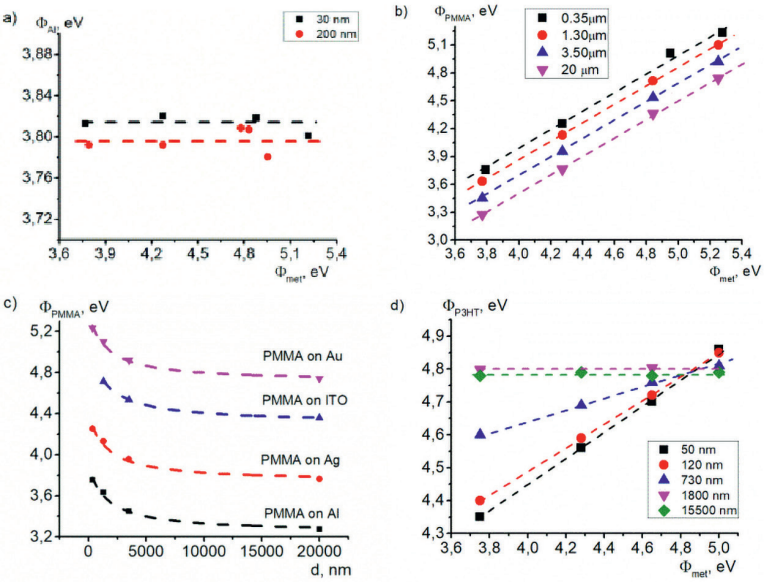

Fig. 4.17 **a) Al work function dependence on metal work function; b) PMMA surface potential dependence on metal work function for samples with various thickness, c) PMMA surface potential dependence on film thickness with various electrodes under the PMMA layer; d) P3HT surface potential dependence on metal work function for samples with various thickness. Dashed lines are guides for eyes**

According to M. Pfeiffer et al., SKP can be applied to dielectric samples if: 1) the capacitance of the sample is larger than the capacitance of the medium between the probe and the sample; 2) the changes of the applied voltage are slow enough to allow the sample to dielectrically relax [75]. Usually these conditions are easily met. However, when the thickness of the sample is 20 μm, its capacitance is so small that the capacitance of the air between the sample and the probe is not negligible anymore and can influence the results. Second, the SKP used in this research is based on so-called "peak-to-peak voltage" principle, where the applied voltage and its direction is changed with the frequency of over 10 kHz. It could be too fast for dielectric material.

In the case of PVK whose electrical conductivity is relatively low (σ_{PVK} = $2{\cdot}10^{-8}$ S/cm), the slope coefficient decreased with the increase of film thickness. Nevertheless, these changes were not great – in the case of 70 nm thick film S = 1, while in the case of 1.8 μm thick film S = 0.82 (see Fig. 4.18).

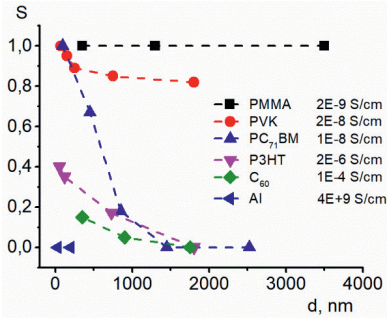

Fig. 4.18 **Slope coefficient S dependence on film thickness for various materials**

For fullerene C_{60} it was possible to obtain a metal-independent surface potential value, similarly as for the Al samples. The thinnest sample (d = 350 nm) had a slope coefficient of S = 0.15. By increasing the film thickness the slope coefficient decreased. For 900 nm thick film S = 0.05, but by doubling the thickness S = 0 was achieved. In the case of $PC_{71}BM$, the slope coefficient changes were more visible – 95 nm thick film S = 1, while for 850 nm film it had decreased to S = 0.18 Further increase in sample thickness (1.45 μm and 2.50 μm) allowed obtaining metal-independent surface potential (see Fig. 4.18). As the measured electrical conductivity for C_{60} was higher than that of $PC_{71}BM$ ($\sigma_{C60} = 1{\cdot}10^{-4}$ S cm^{-1} and $\sigma_{PC71BM} = 1{\cdot}10^{-8}$ S/cm, respectively), the slope coefficient S for C_{60} samples was lower at small sample thickness.

Similarly to the fullerenes, in the case of P3HT a slope coefficient dependence on film thickness was obtained. For 50 nm thick film S = 0.42, and it decreased with the increase of film thickness (see Fig. 4.17 d). As the film

thickness reached 1.8 μm, S = 0 was obtained. Further increase in the film thickness did not change the obtained surface potential, which in this case was Φ_{P3HT} = 4.80 eV. Previous results show that the ionization energy of P3HT is I_{P3HT} = 4.54 eV. It means that the obtained surface potential value is 0.25 eV higher than the ionization energy of P3HT and its relation to the Fermi level of P3HT is questionable. Nevertheless, for all other organic materials, the obtained surface potential values fall in the gap between the ionization energy and electron affinity level of each material.

In Fig. 4.18 a summary of slope coefficient dependence on film thickness for all the studied materials is shown. Two tendencies can be observed. One, with increased film thickness, the slope coefficient decreases and approaches S = 0. The exceptions are PMMA (S stays at 1 for all of the samples) and PVK where slope coefficient stops at the value of around 0.8. Second, as the electrical conductivity of the material increases, S is lower even at thinner films. As the P3HT and fullerene derivatives showed, the film thickness of around 1.5–2 μm is required to obtain S = 0 and to avoid the electrode work function influence on the measured surface potential

4.4.1 Conclusions

For most of the studied materials in the thickness range between 400 nm and 600 nm, a surface potential dependence on metal work function was observed. Only in the case of Al, no such dependence was observed. Dielectric polymer PMMA works as a surface modificator – at fixed film thickness, there is a fixed difference between the surface potential of the sample and metal work function. This could be related to the capacitance effects of the film.

In the case of P3HT electrode-independent surface potential was obtained. Its relation to the Fermi level of P3HT is questionable as it is 0.25 eV higher than the molecule ionization energy, while in all other cases, the obtained surface potential values were between molecule ionization energy and electron affinity level of studied materials.

For organic semiconductors, the surface potential dependence on the metal work function decreased by the increased electrical conductivity of studied material as well as by increased film thickness. Around 1.5–2 μm thick organic semiconductor film is required to obtain a surface potential value that does not depend on metal work function. In that case, the obtained surface potential describes the studied material itself, instead of the metal/organic material system.

THESIS

- Photoelectron yield spectroscopy measurements provide information about the molecule ionization energy of the material even when the obtained film does not fully cover the electrode because the signals of equal amplitude can be separated due to the signal superposition principle. The same superposition principle can be applied in the studies of bulk heterojunction samples.

- Photoelectron yield spectroscopy is a suitable method for energy level studies at the organic compound–organic compound interface in planar as well as in bulk heterojunction systems. In the case of bulk heterojunction samples, the homogenous distribution of the compounds in the bulk of the sample is required.

- In the Kelvin probe measurements, the surface potential dependence on the metal fork function of organic materials is determined by the electrical conductivity of the material as well as the film thickness. For materials with higher electrical conductivity, the lower film thickness is required to reduce the surface potential dependence on metal work function. Films with thickness of 2 μm allow obtaining the metal-independent surface potential value, which can be related to the properties of the studied material itself.

REFERENCES

1. He G (2018). Encycl Mod Opt 5:240–246.
2. Moon D-G (2018). Encycl Mod Opt 5:232–239.
3. Yang F, Kang DW, Kim YS (2017). Sol Energy 155:552–560.
4. To CH, Wong FL, Lee CS, Zapien J a. (2013). Thin Solid Films 549:22–29.
5. Cho AR, Kim EH, Park SY, Park LS (2014). Synth Met 193:77–80.
6. Lee J, Yoshikawa S, Sagawa T (2014). Sol Energy Mater Sol Cells 127:111–121.
7. Albrecht S, Grootoonk B, Neubert S, et al (2014). Sol Energy Mater Sol Cells 127:157–162.
8. Amsalem P, Heimel G, Oehzelt M, Koch N (2015). J Electron Spectros Relat Phenomena 204 A:177–185.
9. Aoki M, Masuda S (2015). J Electron Spectros Relat Phenomena 204:68–74.
10. Feng X, Zhang L, Ye Y, et al (2015). Carbon N Y 87:78–86.
11. Upama MB, Elumalai NK, Mahmud MA, et al (2018). Sol Energy Mater Sol Cells 187:273–282.
12. Gao Y (2010). Mater Sci Eng R Reports 68:39–87.
13. Ishii H, Sugiyama K, Ito E, Seki K (1999). Adv Mater 11:605–625.
14. Jeong J, Lee J, Lee H, et al (2018). Chem Phys Lett 706:317–322.
15. Feng X, Zhao W, Ju H, et al (2012). Org Electron 13:1060–1067.
16. Koch N, Pop D, Weber R, Böwering N (2001). Thin Solid Films 391:81–87.
17. Bröms P, Johansson N, Gymer RW, et al (1999). Adv Mater 11:826–832
18. Opitz A, Frisch J, Schlesinger R, et al (2013). J Electron Spectros Relat Phenomena 190:12–24.
19. Hill IG, Milliron D, Schwartz J, Kahn A (2000). Appl Surf Sci 166:354–362.
20. Gao Y, Ding H, Wang H, Yan D (2007). Appl Phys Lett 91:142112.
21. Heo N, Kim Y, Jung Y, et al (2016). Chem Phys 478:145–149.
22. Tang JX, Lau KM, Lee CS, Lee ST (2006). Appl Phys Lett 88.
23. Frisch J, Vollmer A, Rabe JP, Koch N (2011). Org Electron physics, Mater Appl 12:916–922.
24. Ratcliff EL, Meyer J, Steirer KX, et al (2012). Org Electron physics, Mater Appl 13:744–749.
25. Wei HX, Li YQ, Chen XY, et al (2014). Org Electron physics, Mater Appl 15:2810–2816.
26. Yan C, Wang B, Yu B, et al (2018). Org Electron physics, Mater Appl 62:1–4.
27. Xu Z, Chen L-M, Yang G, et al (2009). Adv Funct Mater 19:1227–1234.
28. Guan Z-L, Kim JB, Wang H, et al (2010). Org Electron 11:1779–1785.
29. Xu Z, Chen L-M, Chen M-H, et al (2009). Appl Phys Lett 95:013301.
30. Tsoi WC, Spencer SJ, Yang L, et al (2011). Macromolecules 44:2944–2952.
31. Kirkus M, Lygaitis R, Tsai M-H, et al (2008). Synth Met 158:226–232.
32. Krucaite G, Tavgeniene D, Xie Z, et al (2018). Opt Mater (Amst) 76:63–68.

33. Lengvinaite S, Grazulevicius J V., Grigalevicius S (2009). Synth Met 159:91–95.
34. Grigalevicius S, Blazys G (2002). Synth Met 128:127–131.
35. Simokaitiene J, Danilevicius A, Grigalevicius S, et al (2006). Synth Met 156:926–931.
36. Baikie ID, Grain A, Sutherland J, Law J (2015). Phys Status Solidi Curr Top Solid State Phys 12:259–262.
37. Harwell JR, Baikie TK, Baikie ID, et al (2016). Phys Chem Chem Phys 18:19738–19745.
38. Honda M, Kanai K, Komatsu K, et al (2007). J Appl Phys 102:103704.
39. Kanai K, Honda M, Ishii H, et al (2012). Org Electron 13:309–319.
40. Machida S, Ozawa Y, Takahashi J ichi, et al (2013). Appl Phys Express 6.
41. Beerbom MM, Lägel B, Cascio a. J, et al (2006). J Electron Spectros Relat Phenomena 152:12–17.
42. Kim JS, Lägel B, Moons E, et al (2000). Synth Met 111:311–314.
43. Nazarov AP, Thierry D (2004). Electrochim Acta 49:2955–2964.
44. Hayashi N, Ishii H, Ouchi Y, Seki K (2003). Synth Met 137:1377–1378.
45. Ohno TR, Chen Y, Harvey SE, et al (1991). Phys Rev B 44:747–755.
46. Kinbara E, Kunugi Y, Harima Y, Yamashita K (2000). Synth Met 114:295–303.
47. Harima Y, Yamashita K, Ishii H, Seki K (2000). Thin Solid Films 366:237–248.
48. Mönch W (1994). Surf Sci 299/300:928–944.
49. Hayashi N, Ito E, Ishii H, et al (2001). In: Synthetic Metals. pp 1717–1718.
50. Ito E, Oji H, Hayashi N, et al (2001). Appl Surf Sci 176:407–411.
51. Ishii H, Hayashi N, Ito E, et al (2004). Phys Status Solidi 201:1075–1094.
52. Schaller RF, Scully JR (2014). Electrochem commun 40:42–44.
53. Williams G, McMurray HN, Newman RC (2013). Electrochem commun 27:144–147.
54. Jo M, Thierry D, Lebozec N (2005). 48:1193–1208.
55. Nazarov A, Vucko F, Thierry D (2016). Electrochim Acta 216:130–139.
56. Schaller RF, Scully JR (2016). Electrochem commun 63:5–9.
57. Baikie ID, Estrup PJ (1998). Rev Sci Instrum 69:3902–3907.
58. Zarins E, Siltane K, Misina E, et al (2012). Proc SPIE 8435:84351Q-84351Q-7.
59. E.A.Silinsh, V.Capek (1994) Organic Molecular Crystals. Interaction, Localization and Transport Phenomena. AIP Press, New York.
60. E.A.Silinsh (1980) Organic Molecular Crystals. Their Electronic States. Springer-Verlag Berlin Heidelberg New York.
61. Scharber MC, Mühlbacher D, Koppe M, et al (2006). Adv Mater 18:789–794.
62. Elumalai NK, Uddin A (2016). Energy Environ Sci 9:391–410.
63. http://www3.nd.edu/~pkamat/pdf/ipce.pdf.
64. Shen T, Tian J, Lv L, et al (2016). Electrochim Acta 191:62–69.
65. Jursenas S, Ggruodis A, Kodis G, et al (1997). SPIE Proc 2968:24–33.
66. Kaulach I, Silinsh EA (1997). Latv J Phys Tech Sci 3:3–10.
67. Dimond NA, Mukherjee TK (1971). Discuss Faraday Soc 51:102.
68. Traskovskis K, Mihailovs I, Tokmakovs A, et al (2012). J Mater Chem 22:11268.
69. Meyerhofer D (1978). J Appl Phys 49:3993.
70. Schlaf R, Murata H, Kafafi Z (2001). J Electron Spectros Relat Phenomena 120:149–154.

71. Sugiyama K, Ishii H, Ouchi Y, Seki K (2000). J Appl Phys 87:295–298.
72. Ozawa Y, Nakayama Y, Machida S, et al (2014). J Electron Spectros Relat Phenomena 197:17–21.
73. Aarnio H, Sehati P, Braun S, et al (2011). Adv Energy Mater 1:792–797.
74. Derry GN, Kern ME, Worth EH (2015). J Vac Sci Technol A 33:060801.
75. Pfeiffer M, Leo K, Karl N (1996). J Appl Phys 80:6880–6883.

AUTHOR'S PUBLICATIONS

Related to the thesis

- **R. Grzibovskis**, A. Vembris, J. Latvels, Photovoltaic properties of glass forming pyranyliden derivatives in thin films, IOP Conf. Ser. Mater. Sci. Eng. 49 (2013). doi:10.1088/1757-899X/49/1/012055.
- E. Zarins, A. Vembris, E. Misina, M. Narels, **R. Grzibovskis**, V. Kokars, Solution processable 2-(trityloxy)ethyl and tert-butyl group containing amorphous molecular glasses of pyranylidene derivatives with light-emitting and amplified spontaneous emission properties, Opt. Mater. (Amst). 49 (2015) 129–137. doi:10.1016/j.optmat.2015.09.004.
- **R. Grzibovskis**, A. Vembris, Study of the P3HT/PCBM interface using photoemission yield spectroscopy, Proc. SPIE. 9895 (2016) 98950Q. doi:10.1117/12.2227823.
- **R. Grzibovskis**, A. Vembris, K. Pudzs, Relation between molecule ionization energy , film thickness and morphology of two indandione derivatives thin films, J. Phys. Chem. Solids. 95 (2016) 12–18. doi:10.1016/j.jpcs.2016.03.010.
- **R. Grzibovskis**, A. Vembris, Energy level determination in bulk heterojunction systems using photoemission yield spectroscopy: case of P3HT:PCBM, J. Mater. Sci. 53 (2018) 7506–7515. doi:10.1007/s10853-018-2050-9.
- **R. Grzibovskis**, A. Vembris, Influence of organic material and sample parameters on the surface potential in Kelvin probe measurements, submitted to *SN Applied Sciences*, first review received.

Unrelated to the thesis

- Grzibovskis R., Vembris A., Sebris A., Kapilinskis Z., Turks M., Energy level determination of purine containing blue light emitting organic compounds, (2018) Proc. SPIE. 10687, art. no. 106871D, DOI: 10.1117/12.2307422.
- Latvels J., Grzibovskis R., Pudzs K., Vembris A., Blumberga D., Photovoltaic effect in bulk heterojunction system with glass forming indandione derivative DMABI-6Ph, (2018) Energy Procedia, DOI: 10.1016/j.egypro.2018.07.073.
- Ruduss A., Traskovskis K., Otikova E., Vembris A., Grzibovskis R., Lielbardis M., Kokars V., 3,3'-Bicarbazole structural derivatives as charge transporting materials for use in OLED devices, (2018) Proceedings of SPIE – The International Society for Optical Engineering, 10687, art. no. 1068718, DOI: 10.1117/12.2306850.
- Pudzs K., Vembris A., Grzibovskis R., Latvels J., Zarins E., Impact of the molecular structure of an indandione fragment containing azobenzene

derivatives on the morphology and electrical properties of thin films, (2016) Materials Chemistry and Physics, 173, pp. 117–125, DOI: 10.1016/j.matchemphys.2016.01.046.
- Pudzs K., Vembris A., Muzikante I., Grzibovskis R., Turovska B., Simokaitiene J., Grigalevicius S., Grazulevicius J.V., Energy structure and electro-optical properties of organic layers with carbazole derivative, (2014) Thin Solid Films, 556, pp. 405–409. DOI: 10.1016/j.tsf.2013.12.031.
- Latvels J., Grzibovskis R., Pudzs K., Vembris A., Blumberga D., Photoelectrical properties of indandione fragment containing azobenzene compounds, (2014) Proceedings of SPIE – The International Society for Optical Engineering, 9137, art. no. 91371G, DOI: 10.1117/12.2052604.
- Latvels J., Grzibovskis R., Vembris A., Blumberga D., Improvement of solar PV efficiency. Potential materials for organic photovoltaic cells, (2013) Environmental and Climate Technologies, 12 (1), pp. 28–33, DOI: 10.2478/rtuect-2013-0013.
- Grzibovskis R., Latvels J., Muzikante I., Photoelectrical properties of thin films of DMABI derivatives, (2011) IOP Conference Series: Materials Science and Engineering, 23 (1), art. no. 012021, DOI: 10.1088/1757-899X/23/1/012021.

PARTICIPATION IN CONFERENCES

- R. Gržibovskis, A. Vembris, Ionization energy or work function determination of materials using photoelectron emission method in institute of Solid state physics, University of Latvia, LU CFI 30. zinātniskā konference, Rīga, 2014. gada 19.–21. februāris, tēzes, 42. lpp.
- R. Grzibovskis, A. Vembris Ionization energy determination of indandione derivatives with various film thickness using photoelectron emission method 10th International Young Scientist Conference „Developments in Optics and Communications" Riga, April 9–12, 2013, Book of Abstracts, p. 26.
- Raitis Grzibovskis, Aivars Vembris, Surface potential, ionization energy, and morphology of organic layer of indandione derivatives with various thickness, SPIE Photonics Europe, April 14–17, 2014, Brussels, Belgium, Technical summaries, p. 333.
- Raitis Grzibovskis, Aivars Vembris, Correlation between ionization energy and surface potential of organic thin films, *Advanced optical materials and devices AOMD-8*, August 25–27, 2014, Riga, Latvia, Book of Abstracts, p. 44.
- Raitis Grzibovskis, Aivars Vembris, Kaspars Pudzs, Dependence of thin film energy level and morphology on its thickness, *10th International Conference on Electroluminescence and Organic Optoelectronics (ICEL-10)*, August 31 – September 3, Cologne, Germany, Conference book, p. 101.
- R. Gržibovskis, A. Vembris, Limiting factors for energy level determination using scanning Kelvin probe tecnique, *LU CFI 31. zinātniskā konference, Rīga,* 2015. gada 24.–26. februāris, tēzes, 45. lpp.
- R. Grzibovskis, A. Vembris, K. Pudzs, Molecule ionization energy dependence on film thickness and morphology of two indandione derivatives, Rīgas Tehniskās universitātes *56. Starptautiskā zinātniskā konference,* 2015. gada 14.–16. oktobris, Rīga, 2015, 32. lpp.
- Raitis Gržibovskis, Aivars Vembris, Robežvirsmas starp divām organiskajām vielām pētīšana ar fotoemisijas kvantu iznākuma spektroskopijas metodi, LU CFI 32. zinātniskā konference, Rīga, 2016. gada 17.–19. februāris, tēzes, 27. lpp.
- Raitis Grzibovskis, Aivars Vembris, Kaspars Pudzs, Molecule ionization energy and morphology dependence on film thickness of two indandione derivatives, 12th International young scientist conference "Developments in Optics and Communications", Riga, March 21–23, 2016, Book of Abstracts p. 6.
- Raitis Grzibovskis, Aivars Vembris, Kaspars Pudzs, Ionization energy studies of P3HT-PCBM interface using photoemission yield spectroscopy,

16th Baltic Polymer Symposium, Klaipeda, Lithuania, September 21–24, Book of Abstracts p. 68.

- Raitis Gržibovskis, Aivars Vembris, Organisko plāno kārtiņu virsmas potenciāla atkarība no metāla elektroda izejas darba kelvina zondes mērījumos, *LU CFI 33. zinātniskā konference* Rīga, 2017. gada 22.–24. februāris, tēzes, 7. lpp.
- Raitis Grzibovskis, Aivars Vembris, Armands Sebris, Zigfrids Kapilinskis, Maris Turks, Energy level determination of purine containing blue light emitting organic compounds, SPIE Photonics Europe 2018, Organic Electronics and Photonics: Fundamentals and Devices, Strasbourg, France, April 22–26, 2018, 10687–47.

ACKNOWLEDGMENTS

The biggest "Thank you!" goes to my scientific supervisor *Dr. phys.* Aivars Vembris for valuable advices and ideas during the work, as well as for the immeasurable patience in the leading me through the whole PhD studies.

Thanks to the head of the laboratory *Dr. phys.* Martins Rutkis, who did not let me relax and urged me to finish the thesis.

I thank *Dr. phys.* Kaspars Pudzs for the SEM images of the samples, as well as for the valuable discussions during the work.

I thank Janis Busenbergs for the help with the issues related to the electronics, Andrey Tokmakov for the help in the work with chemicals, Igors Mihailovs for the help with IUPAC nomenclature.

Big "Thank you!" to all the colleagues of Laboratory of Organic Materials, UL ISSP for the valuable discussions in the laboratory meetings and private conversations, as well as for the warm and friendly working environment.

Thanks to the chemists from the Faculty of Materials Science and Applied Chemistry, Riga Technical University for the synthesis of the studied compounds.

I thank Jennifer Mann from Physical Electronics for the UPS measurements and data.

I thank my family for the support and patience.

Financial support provided by

- ERDF Project No. 2010/0252/2DP/2.1.1.1.0/10/APIA/VIAA/009
- ERDF 1.1.1.1 activity project Nr. 1.1.1.1/16/A/046
- National Research Programme No.2014.10-4/VPP-3/21 (IMIS2)
- Scientific Research Project for Students and Young Researchers Nr. SJZ2015/20 and SJZ2016/20 realized at the Institute of Solid State Physics, University of Latvia

is greatly acknowledged.

"Thank you!" to those, who may be forgotten here, but who have helped me in this work.